SI Appendix

Extreme climate after massive eruption of Alaska's Okmok volcano in 43 BCE and effects on the late Roman Republic and Ptolemaic Kingdom

Joseph R. McConnell, Michael Sigl, Gill Plunkett, Andrea Burke, Woon Mi Kim, Christoph C. Raible, Andrew I. Wilson, Joseph G. Manning, Francis Ludlow, Nathan J. Chellman, Helen M. Innes, Zhen Yang, Jessica F. Larsen, Janet R. Schaefer, Sepp Kipfstuhl, Seyedhamidreza Mojtabavi, Frank Wilhelms, Thomas Opel, Hanno Meyer, Jørgen Peder Steffensen

Corresponding author: Joseph R. McConnell, joe.mcconnell@dri.edu

Contents

Other supplementary materials

1. Dataset S01.xlsx contains ice-core data in Fig. 2 and SI Appendix, Figs. S1, S2, and S3.
2. Dataset S02.xlsx contains tephra data in Fig. 3 and SI Appendix, Fig. S5.

Table S1. DRI_NGRIP2 age scale in both year before 1950 (yb1950) and year (BCE/CE). Shading identifies approximate periods in the NGRIP2 and NEEM cores of high (>3 σ above background) non-sea-salt sulfur concentration indicating elevated volcanic fallout.

yb1950 (ybp)	BCE(-)/CE(+)	Approximate Date
1948	+2	Jan-01
1948.25	+1	Oct-01
1948.5	+1	Jul-01
1948.75	+1	Apr-01
1949	+1	Jan-01
1949.25	-1	Oct-01
1949.5	-1	Jul-01
1949.75	-1	Apr-01
1950	-1	Jan-01
1950.25	-2	Oct-01
1989	-40	Jan-01
1989.25	-41	Oct-01
1989.5	-41	Jul-01
1989.75	-41	Apr-01
1990	-41	Jan-01
1990.25	-42	Oct-01
1990.5	-42	Jul-01
1990.75	-42	Apr-01
1991	-42	Jan-01
1991.25	-43	Oct-01
1991.5	-43	Jul-01
1991.75	-43	Apr-01
1992	-43	Jan-01
1992.25	-44	Oct-01
1992.5	-44	Jul-01
1992.75	-44	Apr-01
1993	-44	Jan-01
1993.25	-45	Oct-01
1993.5	-45	Jul-01
1993.75	-45	Apr-01
1994	-45	Jan-01
1994.25	-46	Oct-01

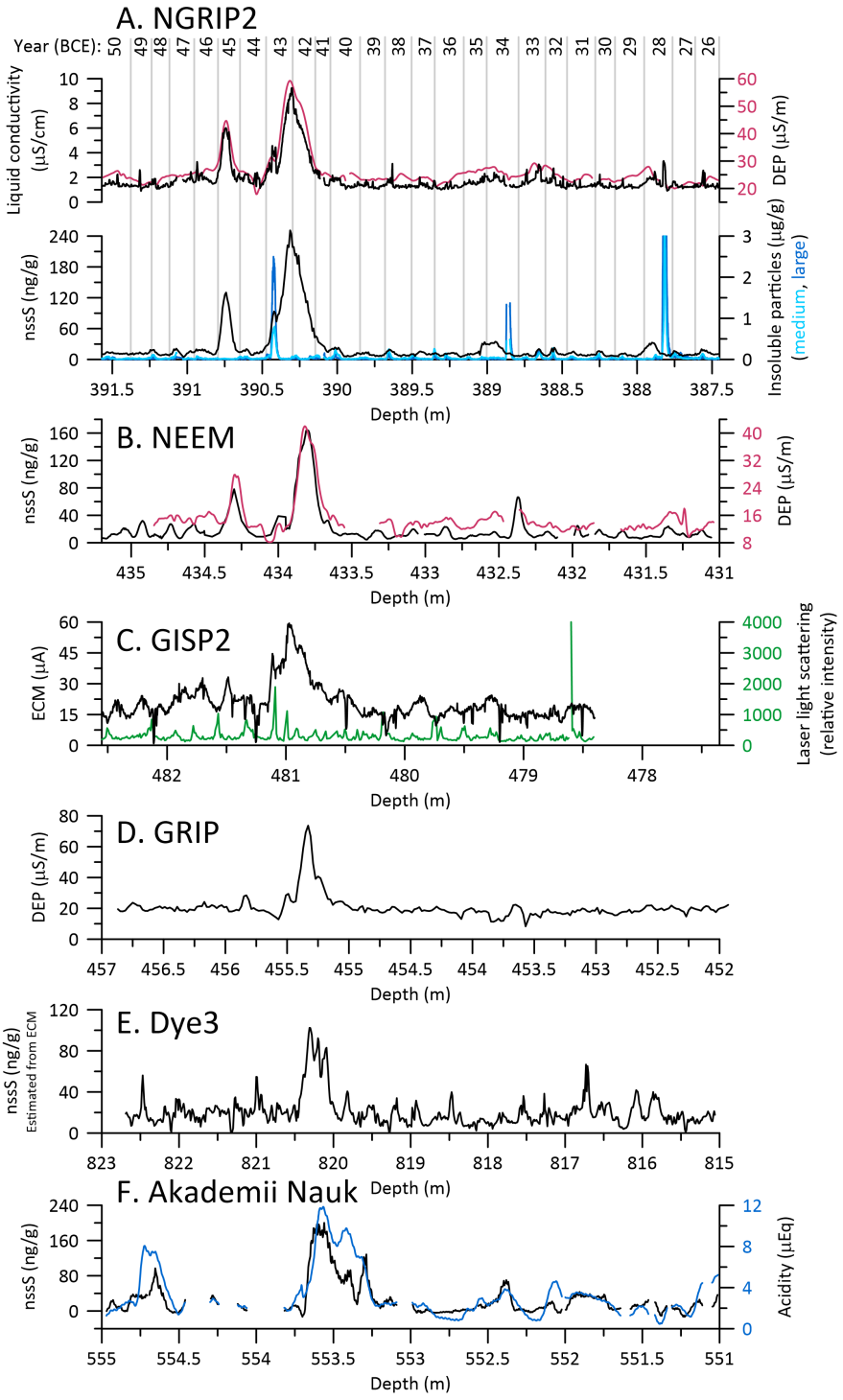

Figure S1. Selected new and previously published measurements of volcanic-fallout-related parameters in the six Arctic ice cores (Fig. 1) evaluated for this study: A. NGRIP2 (this study and (1)), B. NEEM ((1, 2), C. GISP2 (3-5), D. GRIP (6, 7), E. Dye3 (6), and F. Akademii Nauk (this study). Depth ranges correspond approximately to 25 to 50 BCE after synchronization at 43 BCE to the DRI-NGRIP2 age scale (8).

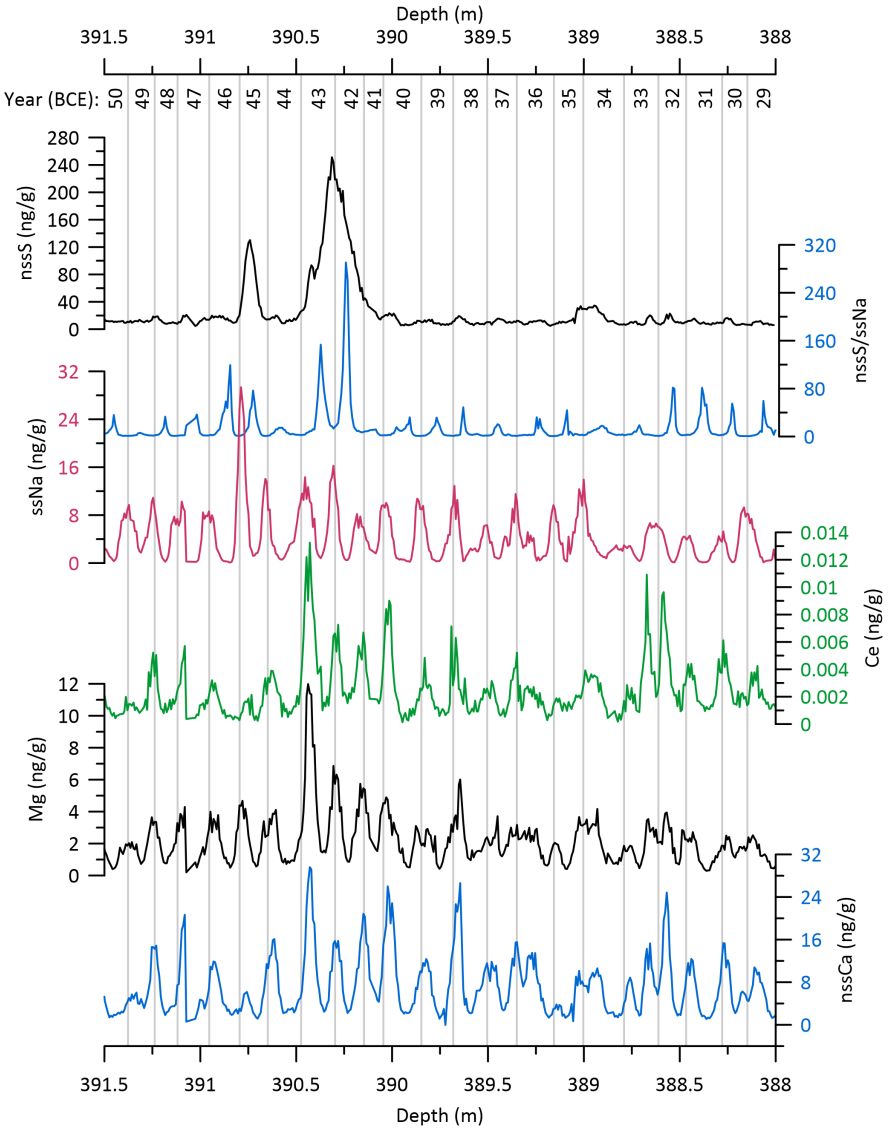

Figure S2. Selected continuous elemental measurements of NGRIP2 ice (388 to 391.5 m) used for annual layer counting. Shown are nssS, the ratio of nssS/ssNa, ssNa, cerium (Ce), magnesium (Mg), and nssCa, where nssS is non-sea-salt sulfur, ssNa is sea-salt sodium, and nssCa is non-sea-salt calcium. Also shown are mid-winter (ostensibly January 1) annual layer picks corresponding to 29 BC to 49 BCE on the DRI_NGRIP2 age scale (8). Ce and nssCa are primarily continental dust indicators while Mg includes both sea-salt and dust components. nssS reflects both volcanic fallout and background marine and terrestrial biogenic emissions.

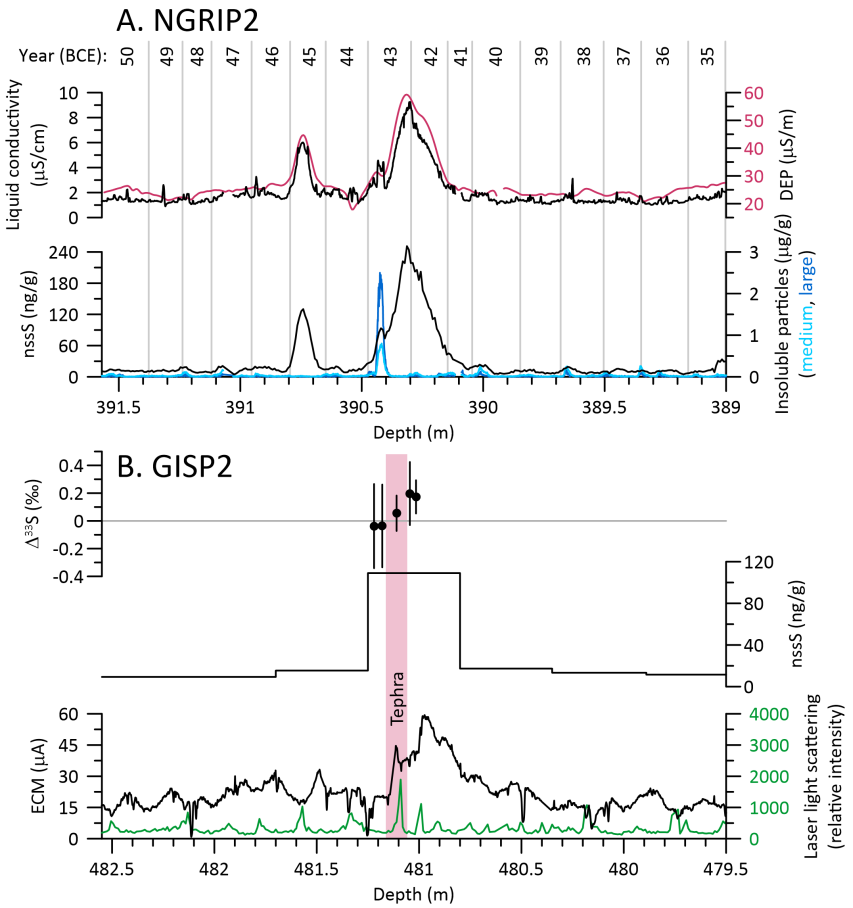

Figure S3. Volcanic fallout surrounding the 43 BCE Okmok II eruption in the A. NGRIP2 and B. GISP2 ice cores. Shown for NGRIP2 are continuous measurements of liquid conductivity (this study), field DEP (1), nssS (this study) and medium (2.5 to 5 µm) and large (5 to 10 µm) insoluble particle counts (this study). Shown for GISP2 are discrete measurements of $\Delta^{33}S$ (±2σ) (this study), discrete sulfate (4), ECM (3), and laser light scattering (9). Tephra used to identify Okmok II as the source eruption were filtered from an ice sample extending from 481.06 to 481.16 m depth (vertical shaded bar) from the GISP2 core.

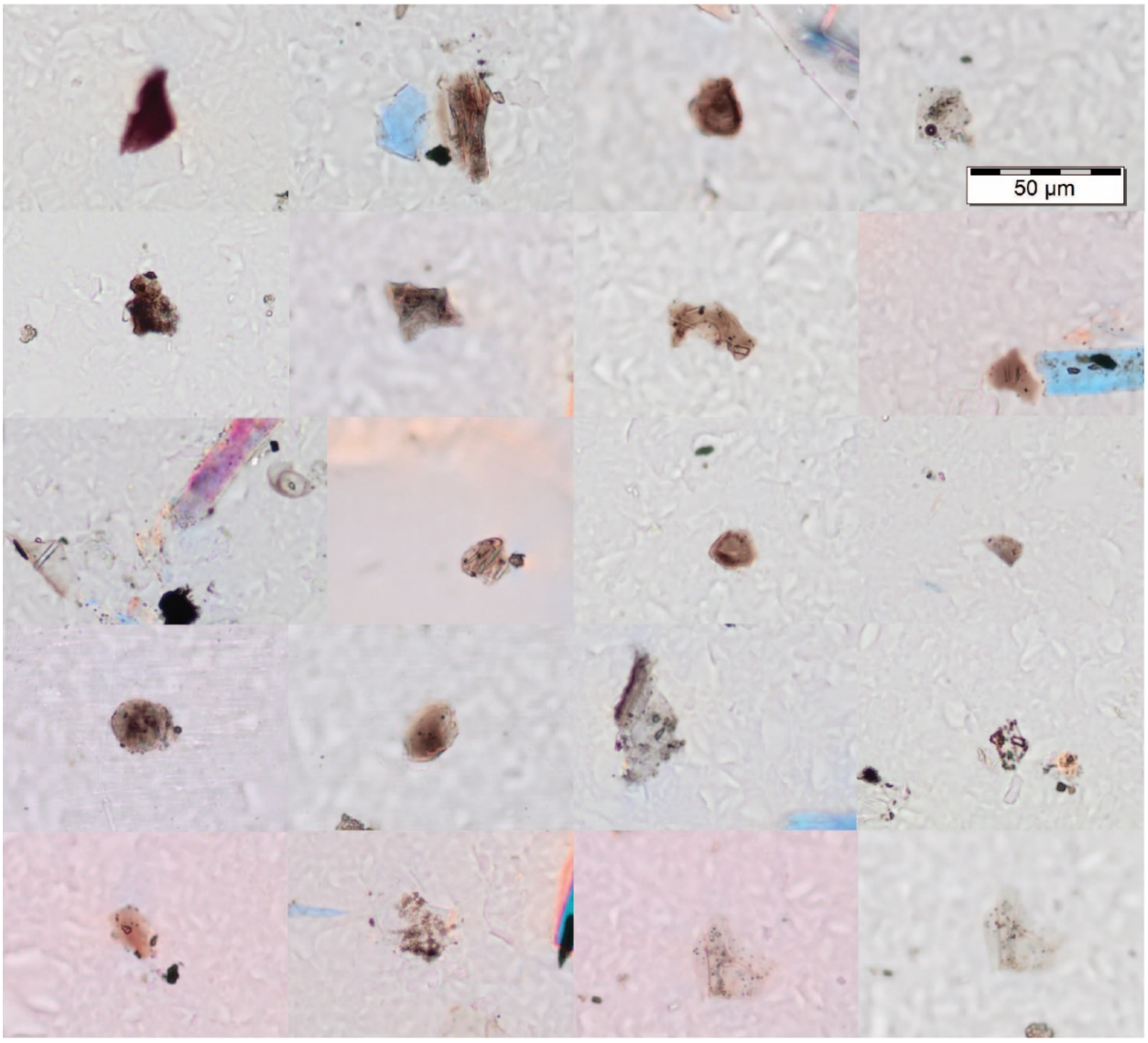

Figure S4. Images of selected tephra shards extracted from GISP2 ice (481.06 to 481.16 m) and geochemically tied to the Okmok II eruption that started in early 43 BCE.

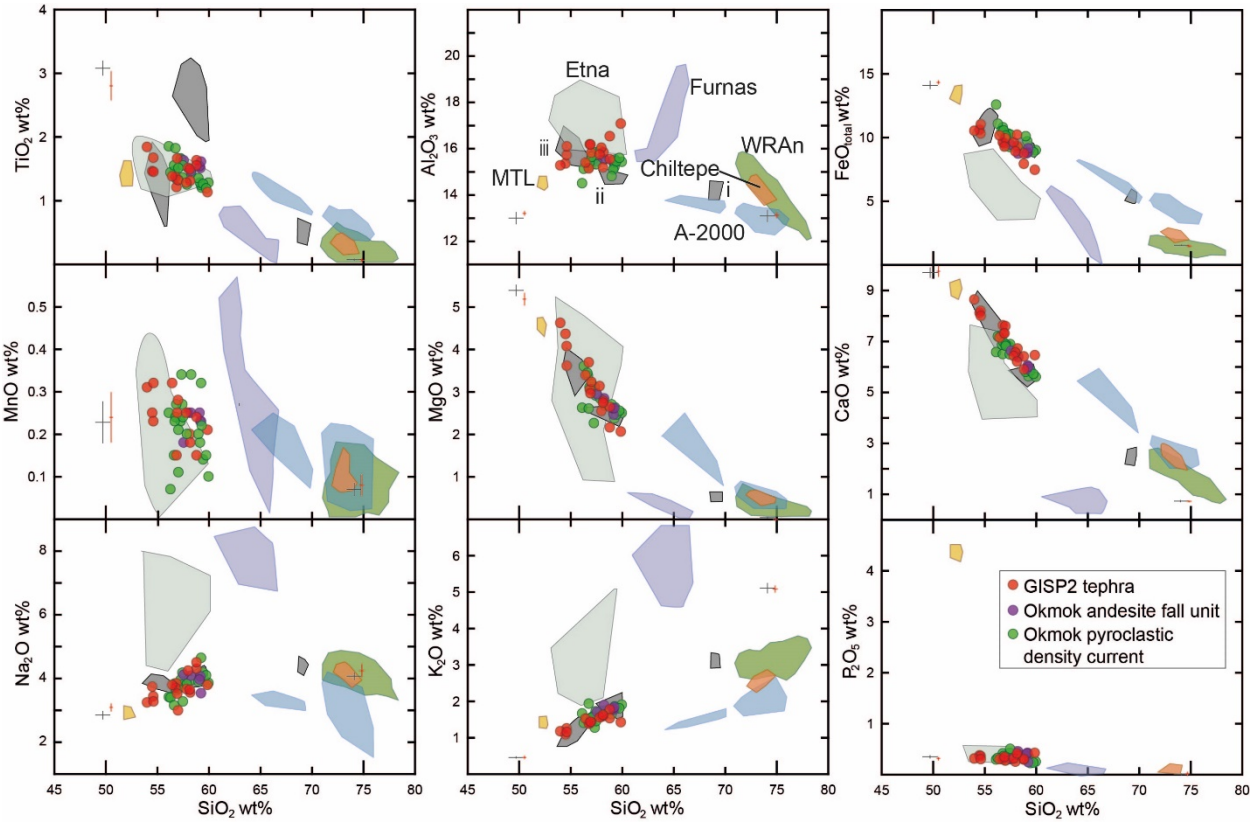

Figure S5. Tephra geochemistry comparisons between shards extracted from GISP2 ice (481.06 to 481.16 m) and potential NH source eruptions including Etna, as well as large eruptions thought within dating uncertainties to have occurred in the 1st century BCE. Filled circles show measurements (this study) of GISP2 and Okmok reference tephra (Materials and Methods; Dataset S02). Shaded regions show tephra reference measurements from other potential source volcanoes: Etna, Italy (10, 11); Chiltepe from Apoyeque, Nicaragua (12, 13); Masaya Triple Tuff (MTL), Nicaragua (12); A-2000, Askja, Iceland (14); White River Ash northern lobe (WRAn), Churchill, Canada (15); Furnas, Azores (16). Gray shading shows prior measurements of tephra samples from the first (i.), second (ii.) and third (iii.) eruption phases of Okmok II (17). Analytical precision for the GISP2/Okmok measurements is illustrated by the red crosses representing 2σ of repeated analyses of the secondary glass standards (high Si – Lipari, low Si - Laki); for comparison, accepted values for Lipari and Laki (2 σ) (18) are shown by the grey crosses.

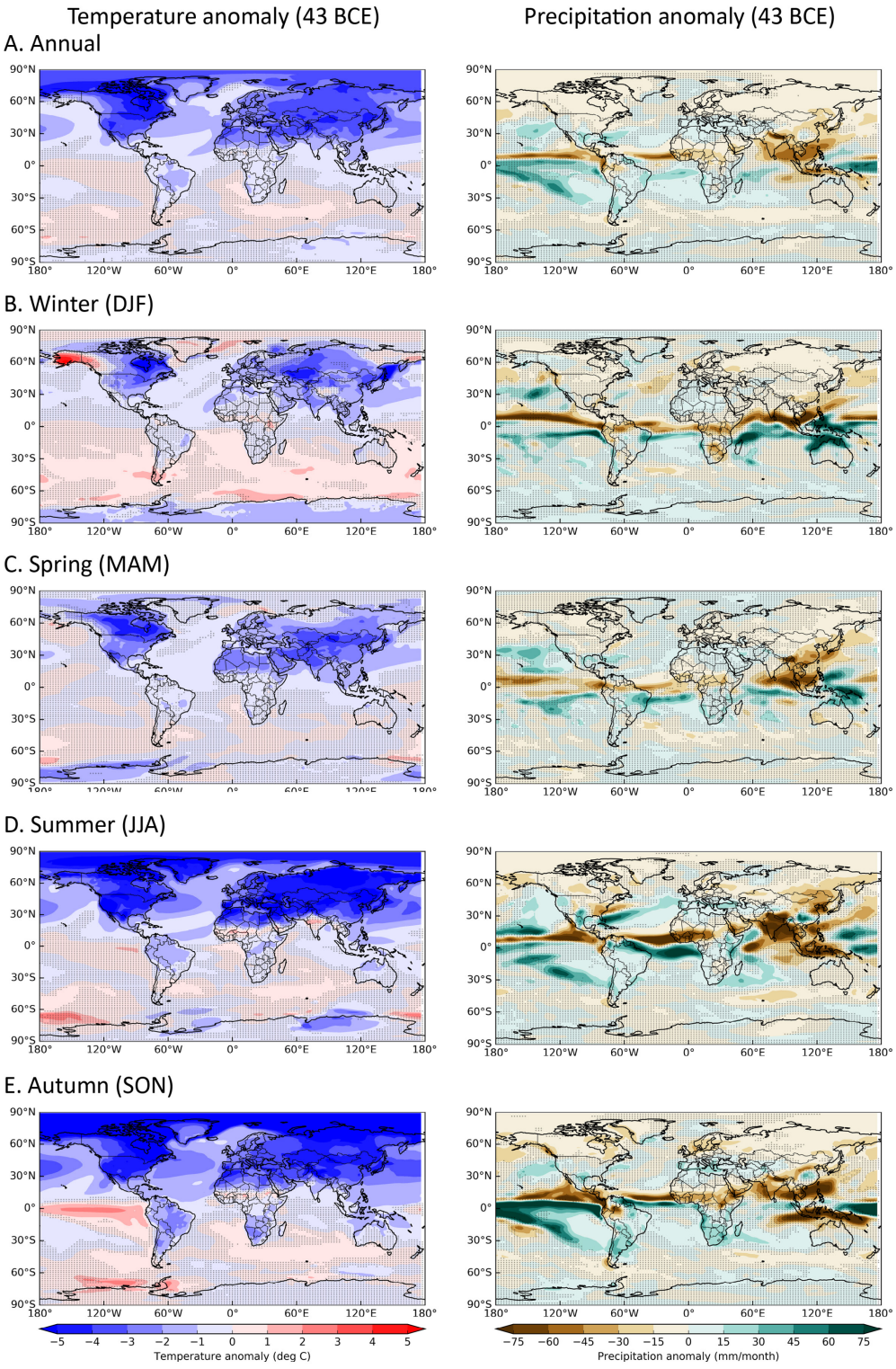

Figure S6. Annual and seasonal 43 BCE CESM-modeled (Materials and Methods) temperature and precipitation anomalies relative to the 60 to 46 BCE reference period with no volcanic forcing. Dots show areas where the anomalies are not significant (2σ) relative to the background variability.

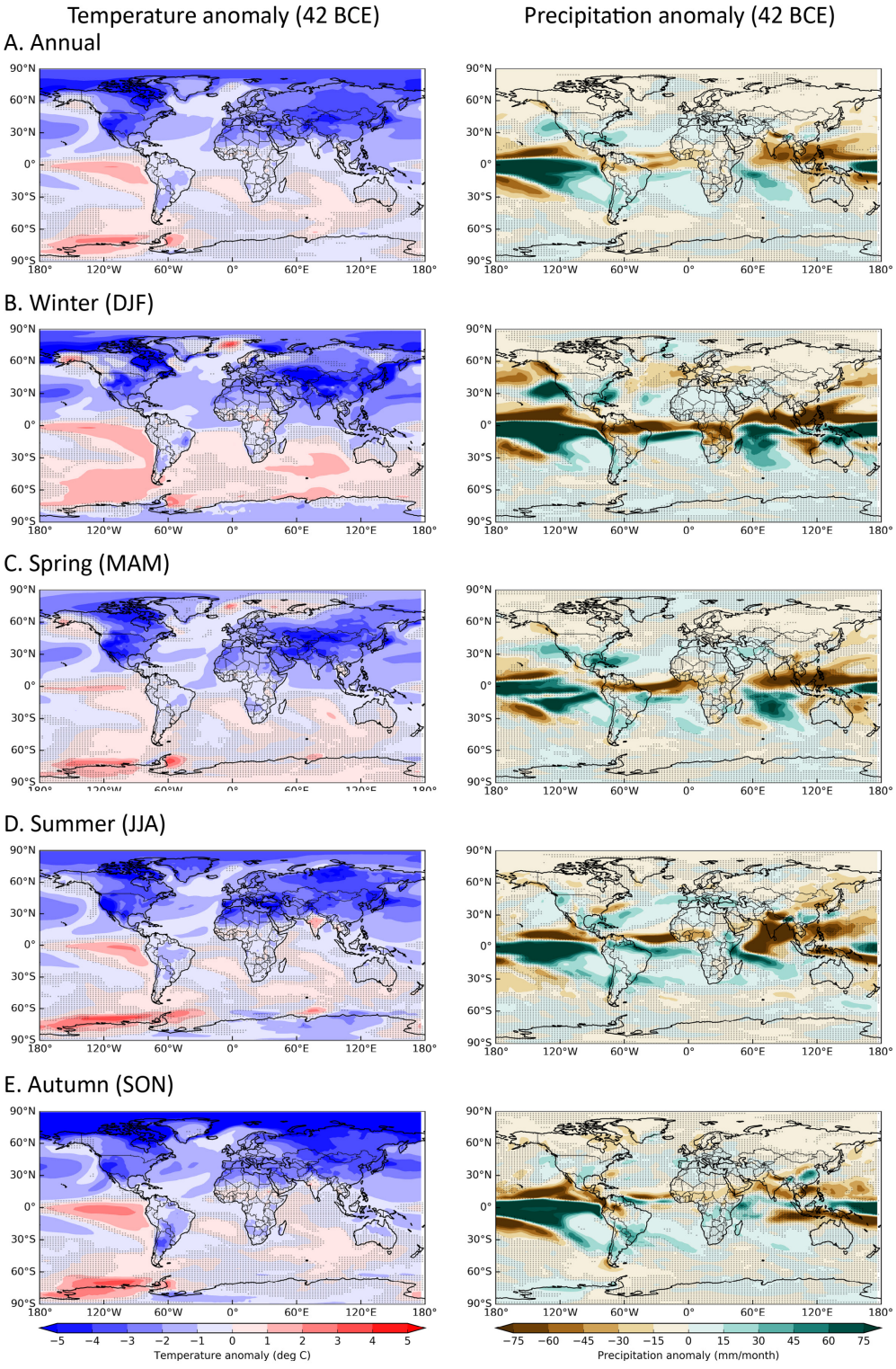

Figure S7. As in SI Appendix, Fig. S6 but for 42 BCE.

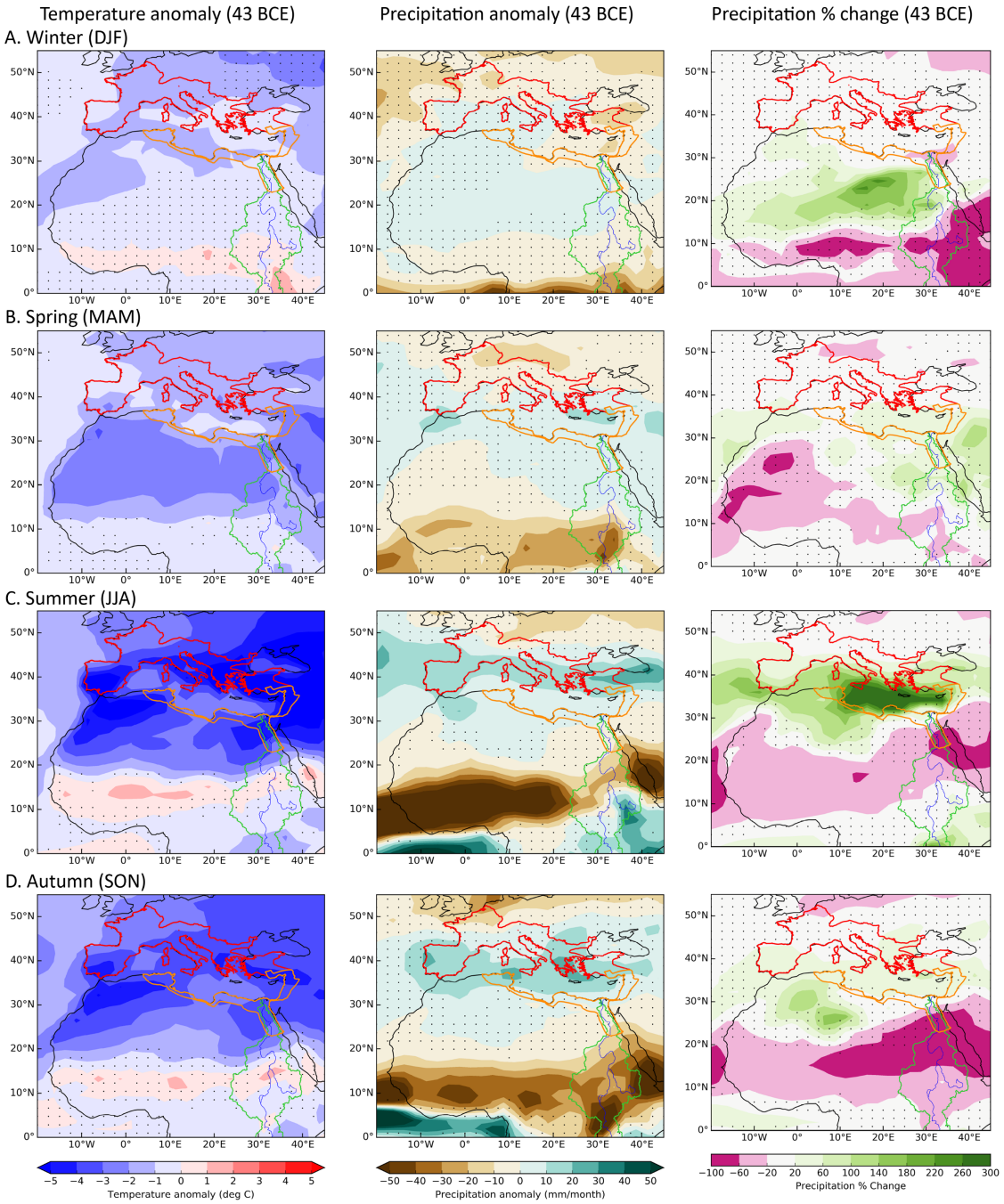

Figure S8. Seasonal 43 BCE CESM-modeled (Materials and Methods) temperature and precipitation anomalies in response to radiative forcing from the early 43 BCE Okmok II eruption. Outlines show (red) Roman provinces north of the Mediterranean, (orange) Ptolemaic Kingdom and Roman provinces south of the Mediterranean, and (green) the Nile River drainage. Anomalies and precipitation change are relative to the 60 to 46 BCE reference period with no volcanic forcing. Dots show areas where the anomalies are not significant (2σ) relative to the background variability.

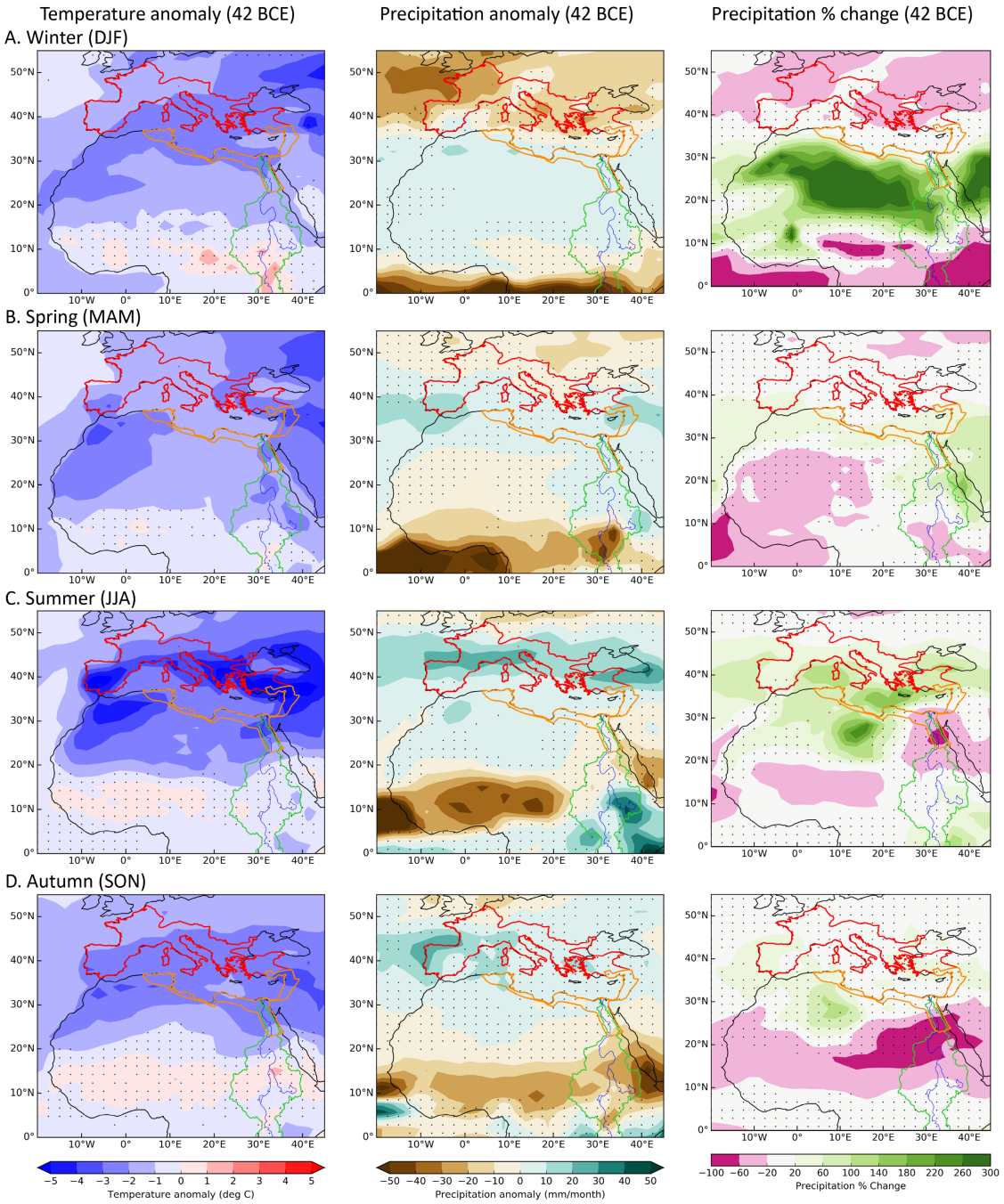

Figure S9. As in SI Appendix, Fig. S8 but for 42 BCE.

Supplemental Information References

1. S. Mojtabavi *et al.*, A first chronology for the East GReenland Ice–core Project (EGRIP) over the Holocene and last glacial termination. *Climate of the Past Discussions* (2019).
2. M. Sigl *et al.*, Timing and climate forcing of volcanic eruptions for the past 2,500 years. *Nature* **523**, 543–549 (2015).
3. K. Taylor, R. Alley, G. Lamorey, P. Mayewski, Electrical measurements on the Greenland Ice Sheet Project 2 core. *Journal of Geophysical Research-Oceans* **102**, 26511-26517 (1997).
4. G. Zielinski *et al.*, Record of volcanism since 7000 B.C. from the GISP2 Greenland ice core and implications for the volcano-climate system. *Science* **264**, 948-952 (1994).
5. G. Zielinski, G. Mershon, Paleoenvironmental implications of the insoluble microparticle record in the GISP2 (Greenland) ice core during the rapidly changing climate of the Pleistocene-Holocene transition. *Geological Society of America Bulletin* **109**, 547-559 (1997).
6. H. Clausen *et al.*, A comparison of the volcanic records over the past 4000 years from the Greenland Ice Core Project and Dye 3 Greenland Ice Cores. *Journal of Geophysical Research-Oceans* **102**, 26707-26723 (1997).
7. E. Wolff, J. Moore, H. Clausen, C. Hammer, Climatic implications of background acidity and other chemistry derived from electrical studies of the Greenland Ice Core Project ice core. *Journal of Geophysical Research-Oceans* **102**, 26325-26332 (1997).
8. J. McConnell *et al.*, Lead pollution recorded in Greenland ice indicates European emissions tracked plagues, wars, and imperial expansion during antiquity. *Proceedings of the National Academy of Sciences of the United States of America* **115**, 5726-5731 (2018).
9. M. Ram, G. Koenig, Continuous dust concentration profile of pre-Holocene ice from the Greenland Ice Sheet Project 2 ice core: Dust stadials, interstadials, and the Eemian. *Journal of Geophysical Research-Oceans* **102**, 26641-26648 (1997).
10. L. Sadori, B. Narcisi, The Postglacial record of environmental history from Lago di Pergusa, Sicily. *Holocene* **11**, 655-671 (2001).
11. H. Vogel, G. Zanchetta, R. Sulpizio, B. Wagner, N. Nowaczyk, A tephrostratigraphic record for the last glacial-interglacial cycle from Lake Ohrid, Albania and Macedonia. *Journal of Quaternary Science* **25**, 320-338 (2010).
12. S. Kutterolf *et al.*, Pacific offshore record of plinian arc volcanism in Central America: 1. Along-arc correlations. *Geochemistry Geophysics Geosystems* **9** (2008).
13. S. Kutterolf, A. Freundt, C. Burkert, Eruptive history and magmatic evolution of the 1.9 kyr Plinian dacitic Chiltepe Tephra from Apoyeque volcano in west-central Nicaragua. *Bulletin of Volcanology* **73**, 811-831 (2011).
14. K. Barber, P. Langdon, A. Blundell, Dating the Glen Garry tephra: a widespread late-Holocene marker horizon in the peatlands of northern Britain. *Holocene* **18**, 31-43 (2008).
15. S. Preece *et al.*, Chemical complexity and source of the White River Ash, Alaska and Yukon. *Geosphere* **10**, 1020-1042 (2014).

16. S. Wastegård, H. Johansson, J. Pacheco, New major element analyses of proximal tephras from the Azores and suggested correlations with cryptotephras in northwest Europe. *Journal of Quaternary Science* **35**, 114-121 (2020).
17. J. Larsen, C. Neal, J. Schaefer, J. Biget, C. Nye, Late Pleistocene and Holocene caldera-forming eruptions of Okmok Caldera, Aleutian Islands, Alaska. *Geophysical Monograph Series* **172** (2007).
18. S. Kuehn, D. Froese, P. Shane, I. INTAV Intercomparison Participants, The INTAV intercomparison of electron-beam microanalysis of glass by tephrochronology laboratories: Results and recommendations. *Quaternary International* **246**, 19-47 (2011).